Jurnal Teknologi

Full Paper

A COMPARATIVE STUDY ON SPECTROGRAM AND S-TRANSFORM FOR BATTERIES PARAMETERS ESTIMATION

Muhammad Sufyan Safwan Mohamad Basir[a*], Abdul Rahim Abdullah[b], Norhashimah Mohd Saad[c]

[a]Faculty of Engineering and Information Technology, MAHSA, 42610 Jenjarom, Selangor, Malaysia
[b]Faculty of Electrical Engineering, UTeM, 76100 Durian Tunggal, Melaka, Malaysia
[c]Faculty of Electronics and Computer Engineering, UTeM, 76100 Durian Tunggal, Melaka, Malaysia

Article history
Received
22 May 2018
Received in revised form
2 January 2019
Accepted
15 January 2019
Published online
18 February 2019

*Corresponding author
muhammadsufyansafwan@mahsa.edu.my

Graphical abstract

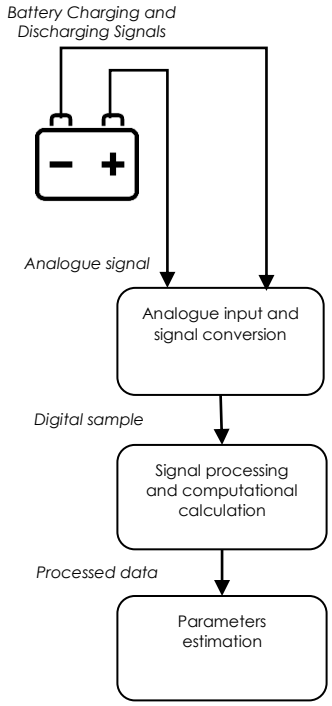

Abstract

This research presents the analysis of battery charging and discharging signals using spectrogram, and S-transform techniques. The analysed batteries are lead acid (LA), nickel-metal hydride (Ni-MH), and lithium-ion (Li-ion). From the equivalent circuit model (ECM) simulated using MATLAB, the constant charging and discharging signals are presented, jointly, in time-frequency representation (TFR). From the TFR, the battery signal characteristics are determined from the estimated parameters of instantaneous means square voltage (V_{RMS} (t)), instantaneous direct current voltage (V_{DC} (t)), and instantaneous alternating current voltage (V_{AC} (t)). Hence, an equation for battery remaining capacity as a function of estimated parameter of V_{AC} (t) using curve fitting tool is presented. In developing a real-time automated battery parameters estimation system, the best time-frequency distribution (TFD) is chosen in terms of accuracy of the battery parameters, computational complexity in signal processing, and memory size. The advantages in high accuracy for battery parameters estimation, and low in memory size requirement makes the S-transform technique is selected to be the best TFD. Then, field testing is conducted for different cases, and the results show that the average mean absolute percentage error (MAPE) calculated is around 4%.

Keywords: Batteries, charging and discharging, time-frequency distribution, parameters estimation

Abstrak

Kajian ini membentangkan analisis bagi pengecasan dan menyahcas isyarat bateri menggunakan teknik analisis spektrum, iaitu periodogram dan taburan masa frekuensi (TMF) iaitu teknik spectrogram dan S-transformasi. Analisis bateri adalah bagi asid plumbum (LA), nikel-logam hidrida (Ni-MH) dan litium-ion (Li-ion). Dari simulasi model litar setara (MLS) menggunakan MATLAB, isyarat berterusan pengecasan dan menyahcas dibentangkan, bersama, dalam perwakilan masa frekuensi (PMF). Melalui PMF, ciri-ciri isyarat bateri ditentukan daripada anggaran parameter voltan punca min kuasa dua serta merta (V_{PMKD} (m)), voltan arus terus serta merta (V_{AT} (m)) dan voltan arus ulang alik serta merta (V_{AU} (m)). Oleh itu, satu persamaan baki kapasiti bateri sebagai fungsi bagi anggaran parameter V_{AU} (m)

menggunakan alat pengukur lengkuk dibentangkan. Dalam membagunkan sistem anggaran parameter bateri automatik semasa, TMF terbaik dipilih dari segi ketepatan parameter bateri, kerumitan pengiraan dalam pemprosesan isyarat dan saiz memori. Kelebihan dalam ketepatan yang tinggi untuk anggaran parameter bateri dan keperluan memori saiz yang rendah menjadikan teknik S-transfomasi dipilih sebagai TMF terbaik. Ketepatan sistem disahkan melalui anggaran parameter menggunakan MLS bagi setiap jenis bateri pada kapasiti yang berbeza. Ujian prestasi menunjukkan bahawa purata min ralat peratusan mutlak (MRPM) adalah sekitar 4%.

Kata kunci: Bateri, pengecasan dan menyahcas, taburan masa frekuensi, anggaran parameter

1.0 INTRODUCTION

The impact of sustainable energy in modern power systems entails the use of battery in energy storage systems. However, poor battery performance not only gives an effect on the load performance, but also on the battery itself [1]. The performance of the battery can be estimated from the measurement of the storage and power capacity. In congruent with the experiment verification made by Hu *et al.* [2], the battery storage capacity showed a 20% drop after 10 years of repeated charging and discharging cycles. In order to maximize the battery run-time, as well as to maintain the power delivered, appropriate actions have to be taken. Therefore, a monitoring system based on battery performance estimation should be developed before effective prevention can be taken [3]. The battery signal, analysis methods, and parameters estimation have been studied according to the Institute of Electrical and Electronics Engineers (IEEE) Standard 1188-2005 standard.

The growing interest in portable equipment requires the use of batteries in daily life. The increased demand for power with high density, and continuity of supply leads to the improvement in battery development from LA, Ni-MH to Li-ion [4]-[6]. With the same working principle which is capability to store, and release energy through the electrochemical process, its performance in terms of energy, voltage and coulomb efficiencies becomes the main concern for applications i.e., electric vehicle, mobile phone, and many others. [7]. This study focuses on secondary battery as the main objective is to analyse battery charging and discharging signal for battery parameters estimation.

A number of studies on battery analysis techniques and signal processing techniques were reported in the literature. Battery analysis techniques i.e., extended Kalman filter (EKF), coulomb counting, and artificial neural network (ANN) were adopted as the performance in terms of accuracy are recognized. EKF failed in meeting the requirement of real-time monitoring system because this technique is a model-based technique that requires predetermined variable to predict the battery state of charge (SOC) [8]. Although the coulomb counting method, and ANN are capable to be implemented in real-time monitoring system, the longer time required in determining the battery capacity becomes its limitation [9]. Moreover, sensitivity in current efficiency due to charging and discharging conditions will affect the performance of these techniques [10].

The common signal processing technique presented by previous researchers in determining the battery parameters is Fourier transform (FT). The limitation of this technique is that it only presents the spectral information (frequency, and not the temporal information (time). Therefore, the changes of battery charging and discharging characteristics cannot be traced. Proposed based of spectrogram was discussed in analysing the signal in marginal joint time-frequency in [11]. The analysis signal was presented in a three-dimensional graph known as time-frequency representation (TFR) that is good in determining the battery performance with respect to time, and frequency. However, the use of fixed window length in the spectrogram greatly affects the resolution of TFR. As an alternative, the wavelet transform was presented with multi-resolution window analysis [12]. The capability of Wavelet transform to focus on good frequency resolution for high frequency components, and good time resolution for low frequency components is needed especially for low frequency components such as for battery application. In order to obtain the precise value at AC and DC components, S-transform is proposed to overcome the limitation of wavelet transform in terms of noise sensitivity. It inherits the element of wavelet transform, and short time Fourier Transform (STFT) in time-frequency spectral localization [13]. Based on the literature, this technique only focuses on applications like radar, and power quality disturbance. Nevertheless, there is a lack of research done on approaches in batteries analysis.

The growing interest in portable equipment requires the use of batteries in daily life. The increased demand of power with high density, and continuity of supply leads to the improvement in battery development from LA, Ni-MH to Li-ion. Repeated cycles of charging and discharging of a

battery, degrade battery performance. The Li-ion has the highest life cycle when applied on photovoltaic energy application [14], but it will be degraded after being used for a long period of time. The failure of the battery to deliver the power source can cause problems like instability in the system, and reduction of load lifetimes which can contribute to economic loss. In handling this issue, proper analysis of battery characteristics is required to ensure that the battery operates under the recommended standard. By displaying the battery characteristics in automated real-time measurement resolves the existing problem such as thermal runaways that can cause fire and explosions [15] as well as enables us to predict problems that may arise. Therefore, analysis technique with high capabilities in low frequency measurement is required in order to solve the battery performance issue.

2.0 METHODOLOGY

2.1 Battery Signal Modelling

Different types of batteries embody different charging and discharging characteristics. This research was carried out using three different types of batteries namely LA, Ni-MH and Li-ion. Equivalent circuit model (ECM) approach was used to generate the charging and discharging signals using MATLAB Simulink. Through this approach, the internal structure of the battery was represented by a single internal resistance following the concept of Rint ECM. This model is capable of giving an accurate prediction of SOC, and state of discharge (SOD) of the battery. Equations of charging and discharging signals of LA, Ni-MH, and Li-ion based on ECM proposed by [16] are defined, respectively as

LA and Ni-MH

$$V_{t,Charging} = E_0 - K\frac{Q}{Q-it}it - K\frac{Q}{it-0.1Q}i - Ri + A \quad (1)$$

$$V_{t,Discharging} = E_0 - K\frac{Q}{Q-it}it - K\frac{Q}{Q-it}i - Ri + A \quad (2)$$

where

$$A = \frac{3}{Q_{\exp}}it\left(-\exp(t) + (V_{full} - V_{\exp})\right) \quad (3)$$

Li-ion

$$V_{t,Charging} = E_0 - K\frac{Q}{Q-it}it - K\frac{Q}{it-0.1Q}i - Ri + B \quad (4)$$

$$V_{t,Discharging} = E_0 - K\frac{Q}{Q-it}it - K\frac{Q}{Q-it}i - R.i + B \quad (5)$$

where

$$B = (V_{full} - V_{\exp})e^{\left(-\frac{3}{Q_{\exp}}it\right)} \quad (6)$$

where V_t is battery terminal voltage, E_0 is battery constant voltage, Q *is* battery capacity, *it* is an actual battery charge, R is battery internal resistance, t is the actual battery current, K is polarization resistance, A is an exponential zone voltage, V_{full} is fully charged voltage, and V_{exp} is exponential zone voltage. The parameters mentioned were obtained from the manufacturer datasheet except K, $3/Q_{exp}$ and V_{full} - V_{exp} should be measured from the discharge curve as in [16].

The polarisation resistance is known to be infinite when it is fully charged. However, experimental results obtained by [17] showed that the contribution of polarisation resistance during the charging process is known to have shifted by 0.1 of the battery capacity. The battery was assumed to be operating with constant nominal capacity, constant internal resistance, no memory effect, no temperature effect, and unlimited cycle life.

2.2 Time Frequency Distributions

For signals with time-varying frequency analysis, using TFDs are recommended [18]. Through the use of TFD, variables t and f are presented together in a three-dimensional plot called TFR, but not mutually exclusive. The constant-f cross-section described the time at present frequency, and constant-t cross section described frequencies present at that particular time [19]. Therefore, estimating the battery parameters using TFDs from multi-frequency components of charging and discharging signals is recommended for fast and accurate estimation. Linear TFDs such as spectrogram and S-transform are discussed in the following section.

2.2.1 Spectrogram

Windowed based STFT was used to achieve the time-localization of the signal. The window length highly depends on the nature of the signal to be analysed as the pitfall of the signals using STFT is the same for all frequency resolutions. Selecting a narrow window length may give the best time resolution, but may end up matching with noise characteristic which can affect the accuracy in measurement. For good frequency resolution, a wider window length is required especially for low frequency analysis that focused on the frequency bands measurement [20, 21]. In signal analysis, square magnitude of the STFT known as spectrogram is commonly used which

provides a distribution of the energy of the signal in time-frequency margin. The spectrogram is calculated as follows:

$$S_x(t, f) = \left| \int_{-\infty}^{\infty} x(t) w(\tau - t) e^{-j2\pi f \tau} d\tau \right|^2 \quad (7)$$

where $x(t)$ is the input analysis signal, and $w(t)$ is the observation window. For the symmetric window, τ is identified as the centre position of the shifted window $w(\tau-t)$. Therefore, appropriate time from the Fourier spectrum of $x(t)w(\tau-t)$ is represented by τ.

A Hanning kernel $w(t)$ with raised cosine function as claimed by [22] which was selected for this study gives narrow effect between fundamental (0 Hz), and other frequency components precisely for spectrogram application with finite window length. Furthermore, spectral leakage can be avoided using Hanning kernel as well as increasing the accuracy in signal analysis [23].

2.2.1 S-Transform

S-transform was proposed to overcome the limitation of STFT in finite window length. The advantage in multi-resolution analysis allowed data to be extracted in the presence of random frequencies [24]. The combination of STFT element in phase and frequency measurements as well as wavelet transform element in progressive resolution showed a promise in complex signal analysis [25].

The time localized variation of individual frequency components using S-transform was captured by frequency dependent Gaussian kernel based on Equation 9. In other words, Gaussian kernel function improved the concentration in measurement through multi-resolution window which relates to the function of time and frequency [26]. The general S-transform is defined in the equations [27] below:

$$ST_x(\tau, f) = \int_{-\infty}^{\infty} x(t) w(\tau - t, f) e^{-j2\pi ft} dt \quad (8)$$

$$w(\tau) = \frac{1}{\sigma\sqrt{2\pi}} e^{\frac{-t^2}{2\sigma^2}} \quad (9)$$

$$\sigma = \frac{1}{|f|} \quad (10)$$

By substituting Equations 9 and 10 into Equation 8, the final expression becomes

$$ST_x(\tau, f) = \int_{-\infty}^{\infty} x(t) \frac{|f|}{\sqrt{2\pi}} e^{-((\tau-t)^2 f^2/2)} e^{-j2\pi ft} dt \quad (11)$$

where $x(t)$ is the signal of interest, $w(t)$ is the scalable Gaussian kernel, and σ is the function of time and frequency which controls the Gaussian kernel position on the x-axis.

2.3 Signal Parameters

Information of the signal for battery parameters estimation was gathered from the TFR based on time, and frequency. From different frequency levels, parameters such as instantaneous of means square voltage (V_{RMS} (t)), instantaneous of direct current voltage (V_{DC} (t)), and instantaneous of alternating current voltage (V_{AC} (t)) are extracted over the time.

2.3.1 Instantaneous of Means Square Voltage

$$V_{RMS}(t) = \sqrt{\int_0^{f_{max}} S_x(t, f) df} \quad (12)$$

where $S_x(t,f)$ is the signal from TFR, and f_{max} is the maximum frequency measured.

2.3.2 Instantaneous of Direct Current Voltage

$$V_{DC}(t) = \sqrt{\int_{f_1 - \frac{\Delta f}{2}}^{f_1 + \frac{\Delta f}{2}} S_x(t, f) df} \quad (13)$$

where f_1 fundamental frequency corresponds to system frequency, and Δf is fundamental frequency bandwidth.

2.3.3 Instantaneous of Alternating Current Voltage

$$V_{AC}(t) = \sqrt{V_{RMS}(t)^2 - V_{DC}(t)^2} \quad (14)$$

2.4 Performance Measurements of Time-Frequency Distributions

TFD techniques were used in analysing signal characteristic in estimating battery capacity. Performance measurements from analysis signal for linear TFD were compared to determine the best TFDs. The performance measurement of the TFD is required to meet the high performance of the signal characteristics. The selection of the best TFD was from the performance measurement of accuracy, computational complexity, and memory size. The criteria of the best TFD encompassed high accuracy, but were low in computational complexity and memory size. Some of the TFD techniques may be low in accuracy, but also has low computational complexity and memory size, and vice versa. Thus, performance analysis for spectrogram and S-transform techniques were performed in this study.

2.4.1 Accuracy of the Analysis

$$MAPE = \frac{100\%}{n} \sum_{t-1}^{n} \left| \frac{A_t - F_t}{A_t} \right| \quad (15)$$

where A_t is the actual value, F_t is the measured value and n is the number of data.

2.4.2 Computation Complexity of the Analysis

$$Cr_{spectrogram} = N - N_w(N_w \log_2(N_w)) \quad (16)$$

where N is the signal length and N_w is window length.

$$Cr_{S-transform} = N - N_w(N_w + N_w \log_2(N_w)) \quad (17)$$

2.4.3 Memory Size of the Analysis

$$Memory_{LinearTFD} = \frac{N_w(N - N_w)}{N_s} \quad (18)$$

where N_S is sample shift.

3.0 RESULTS AND DISCUSSION

This section presents the results of battery charging and discharging signal analysis using spectrogram and S-transform. The charging and discharging signals for LA, Ni-MH, and Li-ion batteries are presented for 5 cycles measured between 0 to 9000 seconds as indicated in Figure 1 to Figure 3. A fixed conversion of charging and discharging cycle is set for every 1800 seconds until 5 battery cycles is achieved. The choice of charging and discharging time, and current is based on the capabilities of the battery to forbear the overcharge, and over discharge that cause cause error in the measurements. In this study, charging and discharging current is set to a fixed value of 1 A for each type of battery. The simulation of the charging and discharging characteristics of the battery for LA, and Ni-MH follow Equations 1, 2, and 3; and for Li-ion Equations 4, 5, and 6 in MATLAB Simulink.

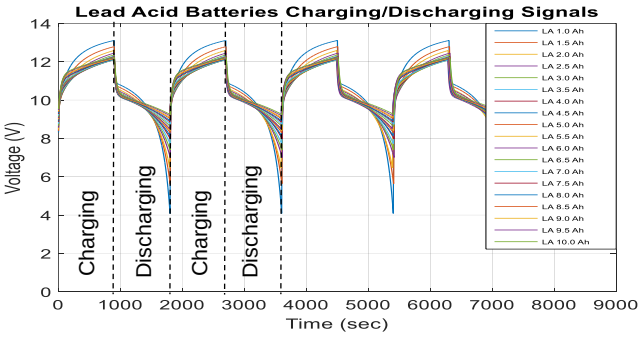

Figure 1 Simulation of voltage charging and discharging signal for 12 V LA batteries

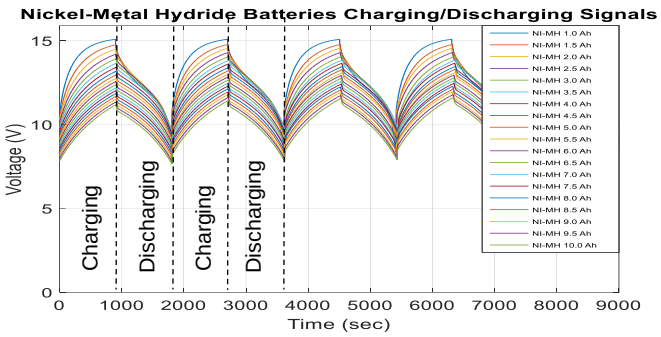

Figure 2 Simulation of voltage charging and discharging signal for 12 V Ni-MH batteries

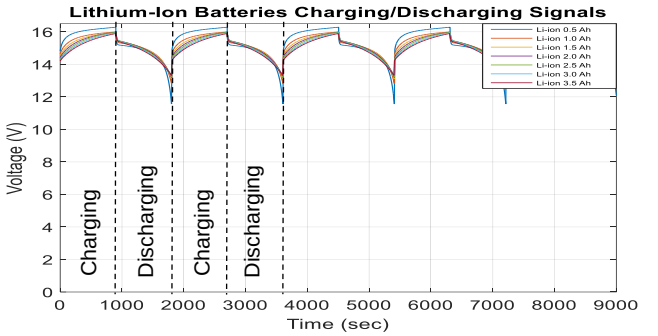

Figure 3 Simulation of voltage charging and discharging signal for 14.8 V Li-ion batteries

From the observation of Figures 1, 2, and 3, different types of batteries give different charging and discharging signals pattern. Selection of batteries with rated voltage of 12 V is crucial as this rated voltage is widely used in many applications such as uninterruptible power supply, robotic and electronic appliances [28]. From the studies of charging and discharging signal with different capacities give information to the battery characteristics as different levels of battery capacities result in different maximum and minimum voltage. Signal processing techniques i.e., spectrogram and S-transform is the best way to extract the battery parameters from the charging and discharging behaviour.

3.1 Time-Frequency Distribution

Analysis of battery charging and discharging signal using spectrogram requires wide window length. In this analysis, the window length is fixed to 4096 that provide good frequency resolution in differentiate the DC and AC components. In this case, the Hanning window is used from the concept of one sample window shift (OSWS). Results of the spectrogram are presented in the three-dimensional plot in of signal energy with respect to time, and frequency. Parameters such as V_{RMS} (t), V_{DC} (t), and V_{AC} (t) are estimated from the TFR using windowed frame of battery signal. This observation window will

cause the TFR graph to appear constant over time duration from 0 to 9000 seconds as shown in Figure 4.

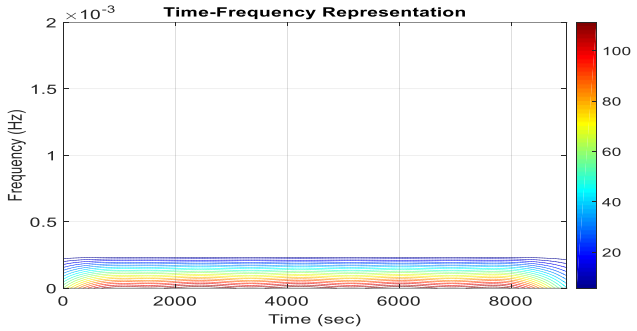

Figure 4 Time-frequency representation using spectrogram

Figure 5 shows TFR obtained using S-transform technique. Multi-resolution Gaussian kernel gives benefit to the TFR in estimating the battery parameters of V_{DC} (*t*), and V_{AC} (*t*) accurately. As can be seen from Figure 5, the parameters for V_{RMS} (*t*), V_{DC} (*t*), and V_{AC} (*t*) are estimated after the TFR is normalized which is between 1000 to 8000 seconds. These phenomena happen because of the use of Gaussian kernel in capturing the signals. Results from the S-transform technique shows that the TFR appears to be good in both f_r and T_r where the characteristics of charging and discharging can still be seen compared to spectrogram (see Figure 4) that appears constant over time.

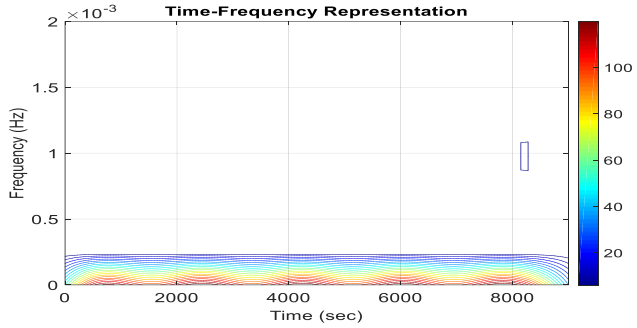

Figure 5 Time-frequency representation using S-transform

In selecting the best TFD, three different criteria namely accuracy, computational complexity, and memory size of the analysis were performed. The results plotted in Figure 6 shows the comparison between spectrogram and S-transform techniques. Accuracy becomes the highest priority in selecting the best TFD that gives reliability in real-time monitoring system to produce an accurate result. Besides, computational complexity also plays a role in providing the battery parameters either in short or long duration of time. The last aspect is memory size that can affect the cost, and size of the system as a high memory size requires high memory space, and better processor performance.

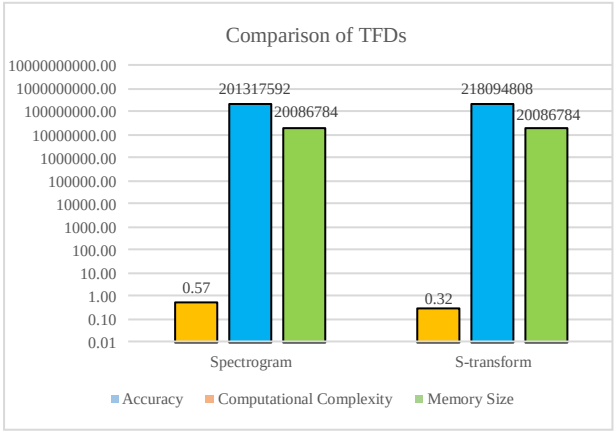

Figure 6 Comparison of the TFDs in terms of accuracy, computational complexit, and memory size of the analysis

Based on Figure 6, the accuracy of spectrogram indicates 0.57% which is 0.26% higher than S-transform. However, the S-transform offers higher computational complexity with an additional 16777216 in signal analysis. Both techniques present the same memory size. In determining the best TFD, high accuracy, low computational complexity, and small memory size are required. Therefore, S-transform is selected to be the best TFD in batteries analysis because S-transfom performs in high accuracy, and low memory size.

3.2 Parameters Estimation of Battery Signals

Parameter estimation using TFDs leads to battery characteristics estimation. The capacity of the battery depends upon the V_{AC} (*t*) value can be numerically identified that gives an advantage to estimate the SOC, and SOD of the battery. From the previous session, S-transform gives the highest accuracy in estimating the battery parameters compared to the spectrogram. Due to this reason, the characteristics of the batteries can be determined precisely using S-transform. Equations 19, 20, and 21 are expressed from the correlation curves (see Figures 7, 8, and 9) simulated using the curve fitting tool. The battery capacity can be calculated from the parameter estimation at AC components using S-transform. This equation is limited to constant charging and discharging current of 1 A.

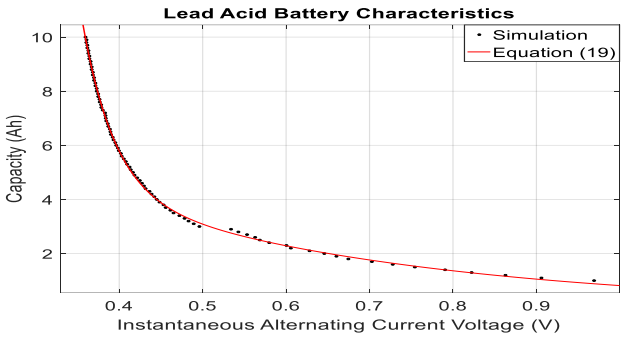

Figure 7 Battery storage capacities from 1.0 Ah to 10.0 Ah of simulation result for LA battery using S-transform

$$Q_{LA.S-transform}(V_{AC}) = 7.234\times10^{4}\exp^{-26.26V_{AC}} + 10.62\exp^{-2.566V_{AC}} \quad (19)$$

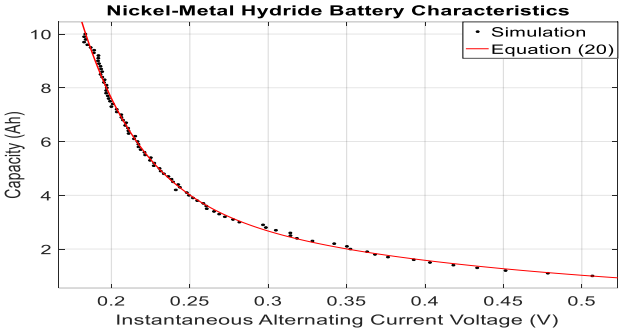

Figure 8 Battery storage capacities from 1.0 Ah to 10.0 Ah of simulation result for Ni-MH battery using S-transform

$$Q_{Ni-MH.S-transform}(V_{AC}) = 752.8\exp^{-26.22V_{AC}} + 8.47\exp^{-4.23V_{AC}} \quad (20)$$

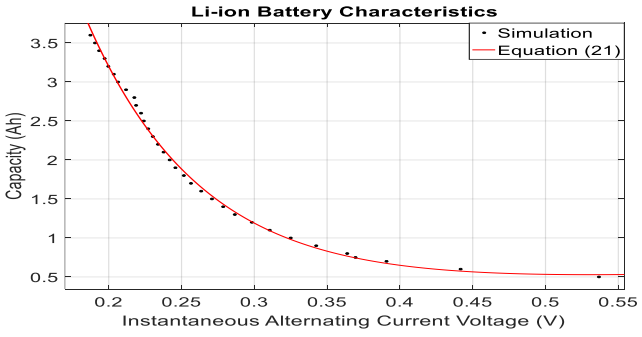

Figure 9 Battery storage capacities from 0.5 Ah to 3.5 Ah of simulation result for Li-ion battery using S-transform

$$Q_{Li-Ion.S-transform}(V_{AC}) = 35.04\exp^{-12.51V_{AC}} + 0.2578\exp^{1.182V_{AC}} \quad (21)$$

3.3 Field Testing

Field testing was done for three different cases for different types of batteries. Based on previous literature, ECM is not superior in terms of accuracy compared to electrochemical model because the errors made by using ECM can hit to 8% [29, 3]. However, due to low in complexity makes ECM is capable to implement in low cost real-time monitoring system. The experiments were conducted by injecting 1 A charging current using adjustable DC power supply model GPC-3030.Then, the battery was discharged using the same amount of current using programmable DC electronic load model 63804.

The experimental charging and discharging signals for battery capacity of 2.3 Ah, 4.5 Ah and 7.2 Ah are shown in Figure 10. During the charging process, the 2.3 Ah battery voltage was higher compared to the other two batteries. The 2.3 Ah battery voltage had a maximum voltage value of 12.58 V after 900 seconds of charging process followed by 12.36 V for a 4.5 Ah battery, and 12.06 V for a 7.2 Ah battery. When the batteries were being discharged, the 7.2 Ah battery voltage was drained by about 3.053 V.

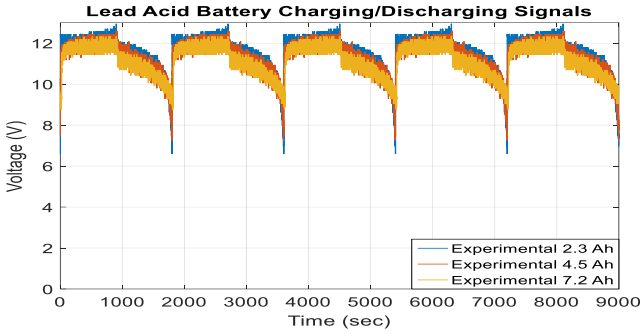

Figure 10 Experimental of voltage charging and discharging signal for 12 V LA with 2.3 Ah, 4.5 Ah and 7.2 Ah batteries

Figure 11 shows the results of charging and discharging signals measured during the experiment for three different battery capacities of 1.3 Ah, 1.8 Ah, and 2.7 Ah, respectively. The charging and discharging signals for the three different battery capacities give the same pattern. Initially, all three Ni-MH batteries voltages experienced sudden increment of 1.7200 V when the charging process is conducted. The voltage for all three cases increased steadily for a certain period of time until the charging process was completed. When the battery was being discharged, the voltage signal for 1.3 Ah battery fell drastically compared to both 1.8 Ah, and 2.7 Ah batteries. Furthermore, it can be clearly seen that the higher the battery capacity, the faster the battery voltage is raised; and the lower the battery capacity the faster the battery voltage is drained.

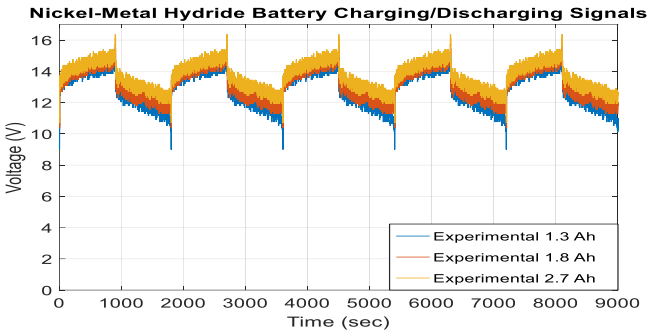

Figure 11 Experimental of voltage charging and discharging signal for 12 V Ni-MH with 1.3 Ah, 1.8 Ah and 2.7 Ah batteries

The experimental charging and discharging for 14.8 V Li-ion batteries with 0.75 Ah, 3.0 Ah, and 3.4 Ah is shown in Figure 12. A fixed conversion of charging and discharging cycle was set for every 1800 seconds for 5 battery cycles. The choice of charging and discharging time, and current are based on the capabilities of the battery to forbear the overcharge, and over discharge that caused inaccurate results. As can be observed, for both charging and discharging signals, the changes are very slow because the characteristics of Li-ion battery are in high power density. Experimental results showed that the differences between 0.75 Ah, 3.0 Ah, and 3.4 Ah charging and discharging signals were due to different battery capacities. During 900 seconds of charging process, the 0.75 Ah battery gives the maximum terminal voltage of 16.12 V followed by 15.62 V for 3.0 Ah, and 15.52 V for 3.4 Ah batteries. Although 3.4 Ah battery gives the lowest maximum voltage during charging process, it does not easily drop during the discharging process. More importantly, it can be clearly seen that the lower the battery capacity, the easier the battery is being charged and discharged.

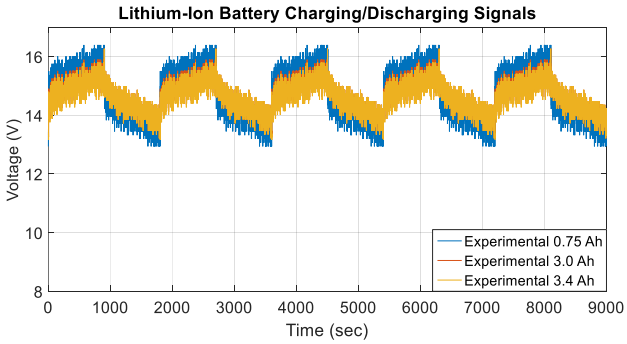

Figure 12 Experimental voltage charging and discharging signal for 14.8 V Li-ion with 0.75 Ah, 3.0 Ah, and 3.4 Ah batteries

For the battery parameters estimation based on the three cases, MAPE was used to validate the results obtained from both simulation, and experimental for V_{RMS} (*t*), V_{DC} (*t*), and V_{AC} (*t*) as in shown in Figure 13. It can be seen that MAPE for V_{RMS} (*t*), V_{DC} (*t*), and V_{AC} (*t*) obtained from LA battery is the highest compared to Ni-MH, and Li-ion batteries. For Li-ion battery, MAPE for overall parameters indicates 3.23%. The accuracy of the experimental is found to be lower than in the simulation because the battery model used neglects many factors such as temperature, internal resistance, and memory effect. Based on the literature, the accuracy in the measurement can be increased by 2% by adding these effects in the battery model.

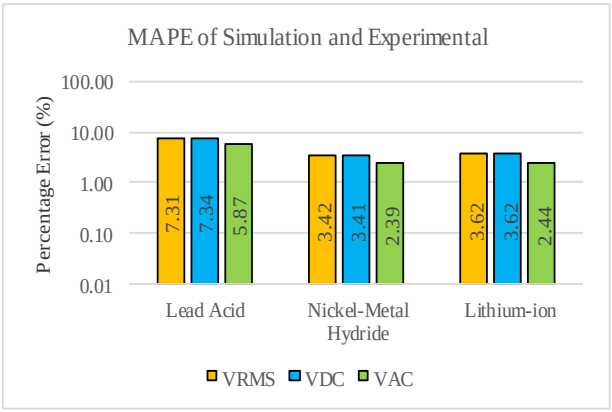

Figure 13 MAPE of simulation and experimental

4.0 CONCLUSION

This research presents the analysis of batteries charging and discharging signals using a TFDs namely spectrogram. and S-transform for batteries parameters estimation. The first part of this article discussed the charging and discharging signals characteristics of LA, Ni-MH, and Li-ion where different types of batteries gives different charging and discharging magnitude. Using TFDs in battery parameters estimation gives benefit in presenting the analysis signal in joint time-frequency domain known as TFR. With the selection of optimum window length that is 4096 in the analysis resulting in high frequency resolution leads to accurate measurement of the signal information.

In selecting the best TFD, both spectrogram and S-transform are being compared in terms of accuracy, computational complexity, and memory size. From the comparison, S-transform is selected due to its advantages which are high in accuracy, and low in memory size. Then, the battery signal characteristics are determined, and equations based on the curve fitting tools are proposed. The proposed technique is capable to estimate the battery parameters namely V_{RMS} (*t*), V_{DC} (*t*), and V_{AC} (*t*) for battery lifetime prediction. For results validation, field testing based on three different cases were conducted for LA, Ni-MH and Li-ion batteries. The analysis for simulation and experimental indicates 4.38% error in average using MAPE. Thus, it can be concluded that the proposed technique is very appropriate to be

implemented for real-time application for batteries parameters estimation.

Nomenclature

LA	Lead acid
ANN	Artificial neural network
ECM	Equivalent circuit model
EKF	Extended Kalman filter
FT	Fourier transform
IEEE	Institute of Electrical and Electronics Engineers
Li-ion	Lithium-ion
MAPE	Mean absolute percentage error
Ni-MH	Nickel-metal hydride
OSWS	One sample window shift
SOC	State of charge
SOD	State of discharge
STFT	Short time Fourier Transform
TFD	Time-frequency distribution
TFR	Time-frequency representation
V_{AC} (*t*)	Instantaneous alternating current voltage
V_{DC} (*t*)	Instantaneous direct current voltage
V_{RMS} (*t*)	Instantaneous means square voltage

Acknowledgement

The authors would like to thank MAHSA University and Universiti Teknikal Malaysia Melaka (UTeM) for providing support and sponsorship for this research.

References

[1] Kasim, R., Abdullah, A. R., Selamat, N. A., Abidullah, N. A., and T. N. S. T. Zawawi. 2015. August. Lead Acid Battery Analysis Using Spectrogram. *Applied Mechanics and Materials*. Trans Tech Publications. 785: 692-696.

[2] Hu, C., Jain, G., Schmidt, C., Strief, C., and Sullivan, M., 2015. Online Estimation of Lithium-ion Battery Capacity Using Sparse Bayesian Learning. *Journal of Power Sources*. 289: 105-113.

[3] Karmore, S. P., Mahajan, A. R., and Kitey, S. 2013. Battery Monitoring and Analysis for Android Based System. In *15th International Conference on Advanced Computing Technologies (ICACT), IEEE*. 1-6.

[4] Bae, K. C., Choi, S. C., Kim, J. H., Won, C. Y., and Jung, Y. C. 2014. LiFePO4 Dynamic Battery Modeling for Battery Simulator. *2014 IEEE International Conference on Industrial Technology (ICIT), IEEE*. 354-358.

[5] Jiang, S. 2011. A Parameter Identification Method for a Battery Equivalent Circuit Model. (No. 2011-01-1367). *SAE Technical Paper*.

[6] Lucas, A., and Chondrogiannis, S., 2016. Smart Grid Energy Storage Controller for Frequency Regulation and Peak Shaving, Using a Vanadium Redox Flow Battery. *International Journal of Electrical Power & Energy Systems*. 80: 26-36.

[7] Brodd, R. J. (ed.). 2012. *Batteries for Sustainability: Selected Entries from the Encyclopedia of Sustainability Science and Technology*. Springer Science & Business Media.

[8] Chen, Z., Fu, Y., and Mi, C. C. 2013. State of Charge Estimation of Lithium-ion Batteries in Electric Drive Vehicles Using Extended Kalman Filtering. *IEEE Transactions on Vehicular Technology*. 62(3): 1020-1030.

[9] Verbrugge, M., and Tate, E. 2004. Adaptive State of Charge Algorithm for Nickel Metal Hydride Batteries Including Hysteresis Phenomena. *Journal of Power Sources*. 126(1): 236-249.

[10] Coleman, M., Lee, C. K., Zhu, C., and Hurley, W. G. 2007. State-of-charge Determination from EMF Voltage Estimation: Using Impedance, Terminal Voltage, and Current for Lead-acid and Lithium-ion Batteries. *IEEE Transactions on Industrial Electronics*. 54(5): 2550-2557.

[11] Holan, S. H., Wikle, C. K., Sullivan-Beckers, L. E., and Cocroft, R. B. 2010. Modeling Complex Phenotypes: Generalized Linear Models Using Spectrogram Predictors of Animal Communication Signals. *Biometrics*. 66(3): 914-924.

[12] Krieger, E. M. 2013. *Effects of Variability and Rate on Battery Charge Storage and Lifespan*. Doctoral Dissertation, Princeton University.

[13] Biswal, M., and Dash, P. K. 2013. Detection and Characterization of Multiple Power Quality Disturbances with a Fast S-transform and Decision Tree based Classifier. *Digital Signal Processing*. 23(4): 1071-1083.

[14] Sullivan, J. L., and Gaines, L. 2010. A Review of Battery Life-cycle Analysis: State of Knowledge and Critical Needs (No. ANL/ESD/10-7). Argonne National Laboratory (ANL).

[15] Wang, Q., Ping, P., Zhao, X., Chu, G., Sun, J., and Chen, C. 2012. Thermal Runaway Caused Fire and Explosion of Lithium Ion Battery. *Journal of Power Sources*. 208: 210-224.

[16] Melentjev, S., and Lebedev, D. 2013, January. Overview of Simplified Mathematical Models of Batteries. *13th International Symposium. Topical Problems of Education in the Field of Electrical and Power Engineering*. Doctoral School of Energy and Geotechnology: Parnu, Estonia. 231-235.

[17] Tremblay, O., and Dessaint, L. A. 2009. Experimental Validation of a Battery Dynamic Model for EV Applications. *World Electric Vehicle Journal*. 3(1): 1-10.

[18] Hou, T. Y., and Shi, Z. 2013. Data-Driven Time–Frequency Analysis. *Applied and Computational Harmonic Analysis*. 35(2): 284-308.

[19] Boashash, B. 2015. *Time-frequency Signal Analysis and Processing: A Comprehensive Reference*. Academic Press. Elservier Ltd. 9.

[20] Kwok, H. K., and Jones, D. L. 2000. Improved Instantaneous Frequency Estimation Using an Adaptive Short-time Fourier Transform. *IEEE Transactions on Signal Processing*. 48(10): 2964-2972.

[21] Pei, S. C., and Huang, S. G. 2012. STFT with Adaptive Window Width based on the Chirp Rate. *IEEE Transactions on Signal Processing*. 60(8): 4065-4080.

[22] Cowell, D. M., and Freear, S. 2010. Separation of Overlapping Linear Frequency Modulated (LFM) Signals using the Fractional Fourier Transform. *IEEE Transactions on Ultrasonics, Ferroelectrics, and Frequency Control*. 57(10): 2324-2333.

[23] Wen, H., Teng, Z., and Guo, S. 2010. Triangular Self-Convolution Window with Desirable Sidelobe Behaviors for Harmonic Analysis of Power System. *IEEE Transactions on Instrumentation and Measurement*. 59(3): 543-552.

[24] Behera, H. S., Dash, P. K., and Biswal, B. 2010. Power Quality Time Series Data Mining Using S-Transform and Fuzzy Expert System. *Applied Soft Computing*. 10(3): 945-955.

[25] Brown, R. A., Lauzon, M. L., and Frayne, R. 2010. A General Description of Linear Time-frequency Transforms and Formulation of a Fast, Invertible Transform that Samples the Continuous S-Transform Spectrum Nonredundantly. *IEEE Transactions on Signal Processing*. 58(1): 281-290.

[26] Biswal, M., and Dash, P. K. 2013. Detection and Characterization of Multiple Power Quality Disturbances

with a Fast S-Transform and Decision Tree Based Classifier. *Digital Signal Processing*. 23(4): 1071-1083.

[27] Abdullah, A. R., Ahmad, N. H. T. H., Abidullah, N. A., Shamsudin, N. H., and Jopri, M. H. 2015. Performance Evaluation of Real Power Quality Disturbances Analysis using S-transform. *Applied Mechanics & Materials*. 752-753: 1343-1348.

[28] Lahyani, A., Venet, P., Guermazi, A., and Troudi, A. 2013. Battery/supercapacitors Combination in Uninterruptible Power Supply (UPS). *IEEE Transactions on Power Electronics*. 28(4): 1509-1522.

[29] Zhang, H., and Chow, M. Y. 2010, July. Comprehensive Dynamic Battery Modelling for PHEV Applications. *IEEE PES General Meeting, IEEE*. 1-6.

[30] Zhu, W. H., Zhu, Y., and Tatarchuk, B. J. 2014. Self-discharge Characteristics and Performance Degradation of Ni-MH Batteries for Storage Applications. *International Journal of Hydrogen Energy*. 39(34): 19789-19798.